Original Research

Revista Brasileira de Física Médica (2026) 20:891

Comparison of methodologies for dosimetric characterization of flattening filter-free (FFF) photon beams in radiotherapy

Camila S. Aguiar[1], Fernanda G. Biagioni[2]

[1]Faculdade de Medicina da Universidade de São Paulo, São Paulo, Brazil
[2]Department of Medical Physics in Radiotherapy, Instituto do Câncer do Estado de São Paulo (ICESP), São Paulo. Brazil

Abstract

The introduction of flattening filter-free (FFF) photon beams in radiotherapy has brought significant benefits, including increased dose rates and reduced treatment delivery times. However, the modification of the dose profile resulting from the removal of the flattening filter limits the direct application of traditional quality control parameters developed for conventional beams. In this scenario, different approaches have been proposed for the dosimetric characterization of FFF beams. In this study, three methodologies described in the literature were evaluated and compared: the Fogliata (FG) method: profile renormalization; the Sharma (SH) method: inflection point; and the Budgell (BDG) method: virtual flattening filter. The analysis was performed for 6 MV FFF and 10 MV FFF photon beams generated by a TrueBeam linear accelerator (Varian Medical Systems, Palo Alto, CA, USA), considering parameters such as symmetry, field size, penumbra, and degree of unflatness. The results demonstrated good agreement among the evaluated methodologies. Differences in penumbra values were below 0.7 mm across all field sizes, and symmetry values remained within 1% for all measurements, complying with recommended tolerances. Field size differences were within ±1.2 mm relative to nominal values, also within established clinical limits. The unflatness parameter showed consistent behavior with literature data, with variations dependent on field size and beam energy. Among the evaluated approaches, the SH method was identified as the most suitable for clinical routine, as it preserves the intrinsic characteristics of FFF beams while providing reliable and consistent dosimetric parameters.

Keywords: Quality Control; flattening filter-free beams; radiotherapy; TrueBeam.

1. Introduction

The evolution of clinical linear accelerators has enabled the use of photon beams with and without a flattening filter. The flattening filter is a conical accessory located in the treatment head, between the primary collimator and the monitor chambers, whose purpose is to produce a uniform dose distribution across the radiation field. However, while effective in achieving flat dose profiles, the presence of the flattening filter results in a reduction of the photon beam dose rate due to radiation absorption, and contributes to increase scatter radiation within the linear accelerator head (1,2).

The consolidation of modern radiotherapy techniques, such as stereotactic radiosurgery (SRS) and stereotactic body radiotherapy (SBRT), which require small irradiation fields and high doses per fraction, has led to the widespread adoption of flattening filter-free (FFF) photon beams in clinical practice. These beams exhibit a non-uniform dose distribution, with a high peak along the central axis, enabling high dose rates and reduced irradiation time (3). This characteristic is particularly useful in hypofractionated treatments and for anatomical regions subject to motion, contributing to greater treatment precision and reproducibility.

However, these same characteristics bring additional challenges for quality control. Standardized and well-established beam parameters, as described in protocols such as the AAPM TG-142 (4), are currently used for the quality control of flattening filter (FF) beams, including flatness, symmetry, and penumbra. Nevertheless, such parameters are not directly applicable to flattening filter-free (FFF) beams. Although various approaches have been proposed for the characterization and quality control of these beams, a standardized protocol for FFF photon beams does not exist yet.

In this context, the aim of this study is to compare different methodologies: i) The Fogliata (FG) method: profile renormalization; ii) The Sharma (SH) method: inflection point; and iii) the Budgell (BDG) method: virtual flattening filter applied to 6 MV and 10 MV FFF beams on a TrueBeam linear accelerator (Varian Medical Systems, Palo Alto, CA, USA), aiming to identify the most suitable methodology for the implementation in the hospitals' routine. (5, 6, 7)

2. Materials and Methods

For data acquisition, inline profiles were obtained using a TrueBeam linear accelerator (Varian Medical Systems, Palo Alto, CA, USA) for 6 MV FFF and 10 MV FFF beams. Measurements were performed in a Blue Phantom water tank (IBA Dosimetry, Schwarzenbruck, Germany) using a CC13 ionization chamber (0.13 cm^3), with a source-to-surface distance (SSD) of 100 cm at a depth of 10 cm. Profiles were acquired with a 0.4 mm step size for 6 cm x 6 cm, 10 cm x 10 cm, 15 cm x 15 cm, 20 cm x 20 cm, 30 cm x 30 cm, and 40 cm x 40 cm field sizes, following the recommendations of the TRS-398 (8) protocol. Data were acquired and processed using the OmniPro-Accept software (IBA Dosimetry, Schwarzenbruck, Germany).

The FFF beams were evaluated through the application and comparison of three methodologies: FH, SH, and BDG methods.

2.1 FG Method: Profile Renormalization

This method, proposed by Fogliata et al. (2012), is based on determining a point on the shoulder of a flattened (FF) beam profile, which is then used to renormalize the FFF beam to the same dose level at that specific point. The shoulder of the profile is located in a region where the dose gradient is smoother, and where both flattened and unflattened beams have similar shapes. Mathematically, this point can be described as the maximum of the third derivative of the FF profile. Thus, FG proposed using a point located in the shoulder region of the FF profile as the normalization point for an FFF profile relative to its corresponding flattened beam (Figure 1).

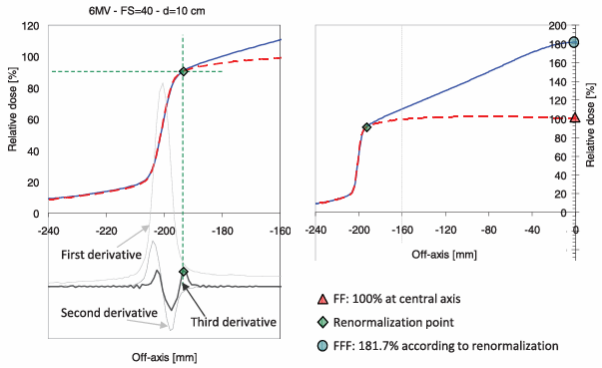

Figure 1. Normalization point obtained through the third derivative of the profile. Source: Fogliata (2012, p. 6457)

According to Fogliata et al. (2012), this point can be determined as the position corresponding to the maximum of the third derivative of the FF beam profile. Operationally, this involves aligning the FF and FFF profiles with respect to the central axis, normalizing the FF beam to 100% at the central axis, and identifying the extrema of the third derivative in the penumbra region. The normalization point is then defined at the off-axis position corresponding to the second maximum (or minimum) closer to the central axis.

In the present study, the normalization factors (NF) previously tabulated in the original article (5) were applied, which depend on field size and measurement depth. These tabulated values are derived based on the same shoulder-point definition described above and were used as a practical and consistent implementation of the method.

After beam normalization, Fogliata et al. (2012) define the following parameters:

Field size: Defined as the distance between the left and right positions corresponding to 50% of the dose on the normalization FFF beam profile. After renormalization, the FFF beam profiles become comparable to a conventional flattened (FF) beam profile, allowing the use of the full width at half maximum (FWHM) concept.

Penumbra: Corresponds to the distance between the 20% and 80% dose levels at the field edge of the renormalized profiles. This correspondence is only valid after the renormalization process, which enables the FFF beams profile to be directly comparable to a conventional flattened beam.

Symmetry: This parameter is defined by Equation 1 below:

$$S = (D_X / D_{-x})_{máx} \quad (1)$$

where D_x and D_{-x} correspond to the dose at coordinates of equidistant points relative to the central axis, and the symmetry corresponds to the maximum value found within the Field Region (FR), such that S ≤ 2%. FR is the area within a defined percentage: for field sizes <10 cm², FR is the area comprised within 60% of the field, and for fields ≥10 cm², the area within 80% of it. (5)

Unflatness: Defined by the ratio between the dose on the central axis and the dose at an off-axis point:

$$U = Dose_{\,eixo\ central} / Dose_{x\ off\text{-}axis} \quad (2)$$

The off-axis point is located at 80% of the field size for fields ≥ 10 cm ^{2} and at 60% for fields <10 cm^2.

2.2 SH Method: Inflection Point

In the method of Sharma et al. (2014), it is not necessary to renormalize the beam; instead, the inflection points (IP) of the profile must be found. This point can be obtained as the midpoint of each side of the high-gradient region of the beam profile, or by plotting the dose difference ΔD (%) between two adjacent measurement points, where the inflection point is the value found in the highest gradient region. The beam parameters defined by Sharma are shown below:

Field Size: The distance separating the inflection points on the right (IP R) and left sides (IP L) of the profile.

Penumbra: Determined based on the dose value at the inflection point (IP) position, described as the Reference Dose Value (RDV). By obtaining points Pa and Pb, located at 1.6 RDV and 0.4 RDV, respectively, the penumbra is obtained through the lateral separation value of the profile between Pa and Pb on each side, yielding the right and left penumbra.

Symmetry: Calculated using Equation (1).

Unflatness: Defined as the lateral distance from the central axis at the 90%, 75%, and 60% dose points on both sides of the axis profile, denoted as $X_{90\%}$, $X_{75\%}$ and $X_{60\%}$.

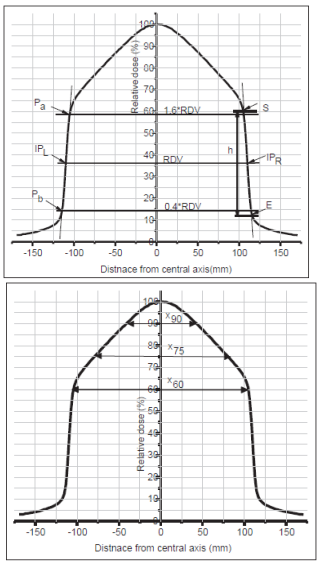

Figure 2. Diagram for determining the inflection point, penumbra, and degree of unflatness. Source: Sharma (2014, p. 209)

2.3 BDG Method: Virtual Flattening Filter

Budgell et al. (2016) normalize FFF field profiles by dividing them by the maximum FFF field 40 cm x 40 cm, resulting in a flat profile. In this way, parameters such as field size, symmetry, and flatness can be measured traditionally, similar to those of flattened (FF) beams (IEC 60976 protocol).

3. Results and Discussion

Figures 3 and 4 below show the profiles obtained for different field sizes with 6 MV FFF and 10 MV FFF beams, respectively. It is observed that for larger fields, the FFF profile exhibits a more pronounced peak at the central axis, whereas for smaller fields, the FFF beam profile approaches a flatter distribution.

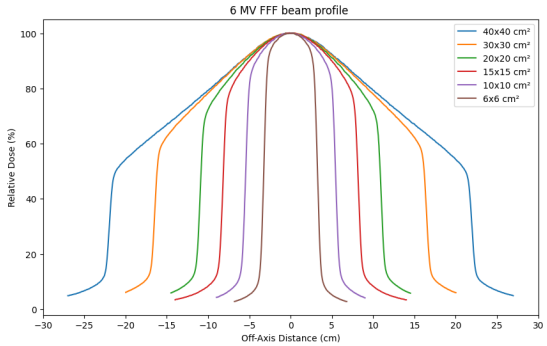

Figure 3. Profiles obtained at 100 cm SSD and 10 cm depth for field sizes of 6 cm x 6 cm, 10 cm x 10 cm, 15 cm x 15 cm, 20 cm x 20 cm, 30 cm x 30 cm and 40 cm x 40 cm, using a 6 MV FFF beam.

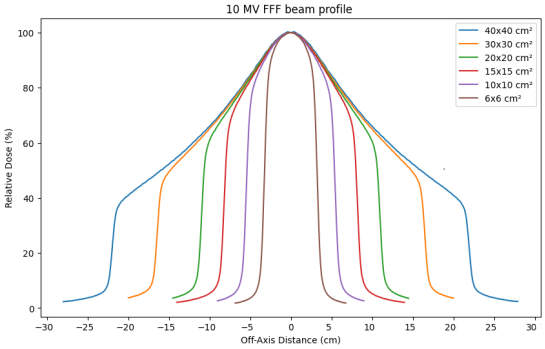

Figure 4. Profiles obtained at 100 cm SSD and 10 cm depth for field sizes of 6 cm x 6 cm, 10 cm x 10 cm, 15 cm x 15 cm, 20 cm x 20 cm, 30 cm x 30 cm e 40 cm x 40 cm, using a 10 MV FFF beam

The results obtained for the parameters of the three methodologies are presented below.

3.1 FG Method

Table 1 presents the normalization factors (NF) obtained for 6 MV FFF and 10 MV FFF energies, based on profiles acquired with different field sizes. It is observed that the NF value increases as the field size grows. This behavior can be explained by the fact that FFF beams exhibit higher intensity in the central region, while becoming approximately flat a few centimeters adjacent to the central axis. Furthermore, the smaller the field size, the flatter the FFF beam profile, resulting in NF values closer to 100%.

It is also verified that the NF increases with beam energy, since higher energies present a steeper dose gradient along the central axis. This effect is related to the Bremsstrahlung photon production process, which generates a more pronounced energy spectrum for higher-energy beams compared to lower-energy ones. (8)

Table 1. Normalization Factor (NF) values for the FG method found for different field sizes and energies of 6 MV FFF and 10 MV FFF.

	6 MV FFF	10 MV FFF
Campo (cm^2)	NF (%)	NF (%)
6 x 6	105.71	109.03
10 x 10	113.18	123.32
15 x 15	123.48	142.58
20 x 20	135.02	163.61
30 x 30	162.90	211.98

Source: The Author (2026).

Figures 5 and 6 present the results of the FG method, comparing dose profiles before and after normalization for 6 MV FFF energy, for field sizes of 20 cm × 20 cm and 6 cm × 6 cm, respectively. For larger field sizes, the 50% positions in FFF beams may extend further from the central axis compared to

FF beams due to the intrinsic peaked shape of FFF profiles prior to normalization. However, the renormalization process minimizes this effect, enabling a consistent definition of field size across different beam types. It is observed that renormalization forces the coincidence of the FFF and FF profiles at the field edge, eliminating the discrepancy caused by the central peak of the FFF beam. Consequently, the relative dose levels represent the same physical positions for both beams, re-establishing the geometric and dosimetric equivalence necessary for the application of traditional parameters such as field size, symmetry, and penumbra.

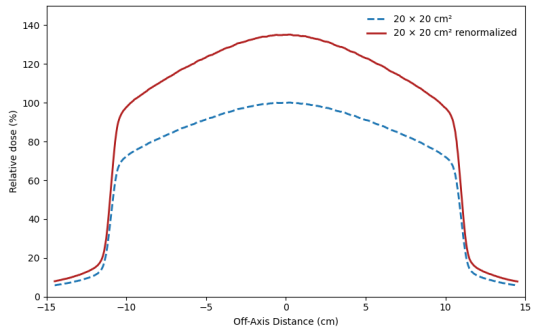

Figure 5. Profiles of the 20 cm x 20 cm field before and after normalization by the FG method's NF factor for the 6 MV FFF beam.

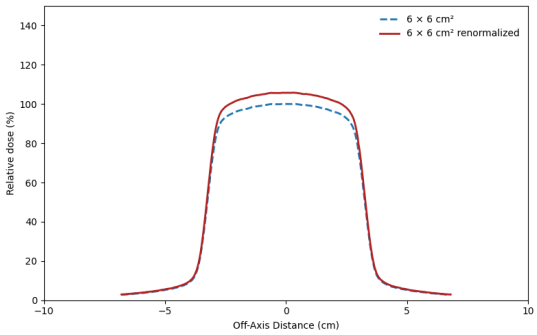

Figure 6. Profiles of the 6 cm x 6 cm field before and after normalization by the FG method's NF factor for the 6 MV FFF beam.

This behavior is consistent with the findings reported by Bueno (2017), who also observed that the degree of central axis peaking in FFF beams increases with field size, while smaller fields tend to exhibit profiles closer to those of conventional flattened beams.

3.2 SH Method

The inflection points determined from each profile are presented in Tables 2 and 3. It is observed that for smaller fields, the inflection point is located closer to the 50% dose level. This behavior is associated with the lower dose gradient along the central axis. As the field size increases, the dose percentage corresponding to the inflection point decreases. For the 20 cm x 20 cm field, the calculated inflection points (IP) correspond to relative dose values (RDV) of 38.90% and 31.80% for 6 MV FFF and 10 MV FFF energies, respectively, with the RDV decreasing as energy increases.

Table 2. Values for the left inflection point (IP L) and right inflection point (IP R), and their respective reference dose values (RDV) for different field sizes and 6 MV FFF beams.

6 MV FFF				
Field size (cm^2)	IP L (cm)	RDV L (%)	IP R (cm)	RDV R (%)
6x6	-3.27	48.3	3.26	49.55
10x10	-5.46	47.85	5.46	47.95
15x15	-8.23	42.80	8.20	45.2
20x20	-11.00	38.90	10.98	40.5
30x30	-16.47	34.50	16.47	34.3

Source: The Author (2026).

Table 3. Values for the left inflection point (IP L) and right inflection point (IP R), and their respective reference dose values (RDV) for different field sizes and 10 MV FFF beams.

10 MV FFF				
Field size (cm^2)	IP L (cm)	RDV L (%)	IP R (cm)	RDV R (%)
6x6	-3.26	46.3	3.26	46.8
10x10	-5.47	42.9	5.47	42.5
15x15	-8.22	36.3	8.21	37.40
20x20	-11.0	31.80	10.99	32.10
30x30	-16.46	25.80	16.49	26.50

Source: The Author (2026).

Figure 7 presents the plot highlighting the inflection points identified for the 20 cm x 20 cm field of the 6 MV FFF beam. It can be observed that the inflection points are located near the midpoint of the high-gradient region of the profile, on both the right and left sides. Furthermore, Figure 8 illustrates the procedure used to determine the unflatness values for the same beam profile. These values correspond to the lateral distances from the central axis at the, 90%, 75%, and 60% dose levels, providing a quantitative assessment of the beam's off-axis dose variation.

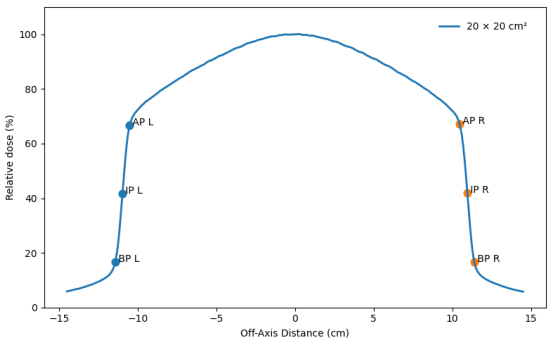

Figure 7. Profile of the 20 cm x 20 cm field with its respective right inflection point (IP R) and left inflection point (IP L), and the points AP R, AP L, BP R e BP L, located at 1.6RVD and 0.4RDV, where RDV is the Reference Dose Value, for the 6 MV FFF beam.

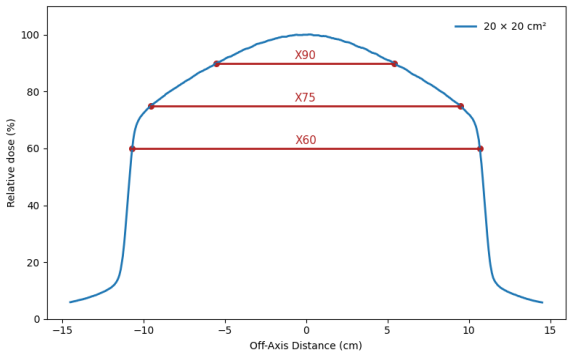

Figure 8. Profile of the 20 cm x 20 cm field showing the lateral distance from the central axis at the 90%, 75%, and 60% dose levels on both sides of the axis, $X_{90\%}$, $X_{75\%}$ e $X_{60\%}$, for the 6 MV FFF beam.

This behavior agrees with the observations of Sharma et al. (2014), who reported that the inflection point shifts toward lower dose levels for larger fields due to the increased central axis peak characteristic of FFF beams.

3.3 BDG Method

Figure 9 presents the application of the BDG method for a 20 cm × 20 cm field size and a 6 MV FFF beam. Figure 9-A displays the dose profiles of the 6 MV FFF beam for the 20 cm × 20 cm and 40 cm × 40 cm fields, while Figure 9-B shows the result of the division between these profiles, highlighting the virtually flattened 20 cm × 20 cm field. The effectiveness of this method in virtually simulating the effect of a flattening filter can be evaluated.

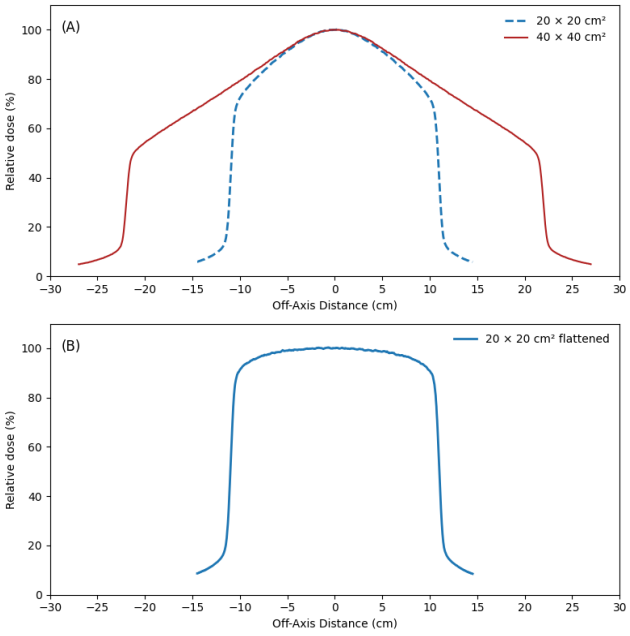

Figure 9. Plot of the 20 cm x 20 cm field using the BDG method for the 6 MV FFF beam. In (A), the FFF beam profile is divided by the 40 cm x 40 cm FFF beam profile, resulting in (B), a flattened 20 cm x 20 cm profile .

By normalizing the FFF beam profile with respect to the largest field size (40 cm × 40 cm), a virtually flattened profile was obtained, allowing the application of conventional definitions of field size and penumbra. These findings confirm the validity and reproducibility of the BDG method for practical dosimetric characterization of FFF beams. When using these approaches, all of which ensure the field edges of FF and FFF beams superimpose and match at 50%, then the standard definition of beam penumbra (20 - 80%) can be used.

3.4 Evaluation of the parameters for each methodology

3.4.1 Penumbra

Table 4 presents the penumbra values calculated using the FG, SH, and BDG methodologies. A good agreement among the three approaches is observed when comparing results obtained from the same beam profiles, with a maximum difference of 0.7 mm between methods. Additionally, the penumbra increases proportionally with increasing field size, consistent with the expected broadening of the geometric and dosimetric field edges for larger irradiation fields.

Table 4. Penumbra values obtained for different methodologies across various field sizes for 6 MV FFF and 10 MV FFF beams, including the maximum difference between methodologies.

	Field size (cm²)	FG (cm)	SH (cm)	BDG (cm)	Max Diff (cm)
6 MV FFF	6 x 6	0.60	0.62	0.62	0.03
	10 x 10	0.68	0.74	0.71	0.06
	15 x 15	0.75	0.81	0.79	0.04
	20 x 20	0.79	0.85	0.84	0.06
	30 x 30	0.94	0.97	0.99	0.05
10 MV FFF	6 x 6	0.65	0.66	0.67	0.04
	10 x 10	0.70	0.72	0.75	0.05
	15 x 15	0.74	0.77	0.79	0.05
	20 x 20	0.78	0.81	0.84	0.06
	30 x 30	0.85	0.92	0.91	0.07

Source: The Author (2026).

The penumbra values reported in the literature exhibit variations that can be attributed to experimental factors, such as the measurement setup, detector type, step size, and acquisition speed. Bellon et al. (2014) performed measurements using a CC13 chamber (0.13 cm³), with an SSD of 100 cm and a depth of 10 cm, on a TrueBeam linear accelerator. For a 10 cm × 10 cm field, they obtained penumbra values of 6.96 mm for the 6 MV FFF beam and 6.98 mm for the 10 MV FFF beam. Similarly, Bueno (2017) reported penumbras of 7.0 mm and 8.0 mm for 6 MV FFF and 10 MV FFF beams, respectively, for a 10 cm × 10 cm field size using different methodologies. These results are consistent with the values found in this study, where the penumbra ranged between 6.8 mm and 7.5 mm for

the 10 cm × 10 cm field at 6 and 10 MV FFF energies. Thus, the comparison of these results with literature data indicates satisfactory agreement.

3.4.2 Symmetry

Table 5 presents the symmetry values obtained using the FG, SH, and BDG methodologies for different field sizes and beam energies. All measured symmetry values were below 1% for both 6 MV FFF and 10 MV FFF beams, regardless of the methodology applied. These results are therefore within stricter tolerances than those recommended by the AAPM TG-142 protocol and are also consistent with literature references. (5, 15)

Table 5. Symmetry values obtained for different methodologies across various field sizes for 6 MV FFF and 10 MV FFF beams.

	Field size (cm^2)	FG (%)	SH (%)	BDG (%)
6 MV FFF	6 x 6	0.81	0.74	0.81
	10 x 10	0.54	0.49	0.57
	15 x 15	0.38	0.39	0.44
	20 x 20	0.81	0.70	0.85
	30 x 30	0.68	0.69	0.80
10 MV FFF	6 x 6	0.62	0.62	0.67
	10 x 10	0.59	0.59	0.67
	15 x 15	0.47	0.48	0.49
	20 x 20	0.65	0.65	0.74
	30 x 30	0.52	0.54	0.54

Source: The Author (2026).

Although small variations between methodologies can be observed, these differences remain below 0.2% in all cases and are attributed to intrinsic differences in the definition and calculation of symmetry for each method, rather than to measurement uncertainty or beam instability. For example, the largest variation between methods was observed for the 20 cm × 20 cm field, where symmetry values ranged from 0.74% (SH) to 0.85% (BDG), still well within acceptable limits. Therefore, the differences observed between methodologies do not represent clinically significant discrepancies and do not compromise the selection of a method for routine quality control. Instead, they reflect the mathematical and geometrical approaches inherent to each methodology. These findings are in agreement with Bueno (2017), who reported symmetry values below 1% across different evaluation methods.

3.4.3 Field Size

Table 6 presents the field size values obtained for each methodology, as well as the differences between the nominal field sizes and the calculated values for each energy and field size analyzed. According to the AAPM TG-142 protocol, the recommended tolerance for symmetric fields is ±2 mm, thus, all obtained results are within the established limit. (5) In general, the results proved to be close to the tolerances reported in the literature by Clivio et al. (2014), where a tolerance of up to 1 mm was obtained for different field sizes in FFF beams from TrueBeam linear accelerators.

3.4.4 Unflatness

Tables 7 and 8 show the unflatness degree values, utilizing the unflatness definitions proposed by Fogliata et al. (2012) and Sharma et al. (2014), respectively. The unflatness parameter was calculated using the FG definition for the normalized beam. Conversely, for the SH definition, the unflatness calculation was performed on the non-normalized beam (SH).

In comparison with Fogliata et al. (2012), the largest unflatness difference found was 0.7 % for the 30 cm x 30 cm field at 6 MV FFF energy. For smaller field sizes, the differences were lower, remaining below 0.5 %, indicating a high level of consistency.

When comparing the analyzed data with Bueno (2017), differences of 0.4% and 0.07% were found for the 10 cm x 10 cm and 20 cm x 20 cm fields, respectively, at 6 MV FFF energy.

Table 7. Unflatness values obtained using the FG methodology for different field sizes and 6 MV FFF and 10 MV FFF beams.

	Field size (cm^2)	FG
6 MV FFF	6 x 6	1.153
	10 x 10	1.219
	15 x 15	1.346
	20 x 20	1.499
	30 x 30	1.820
10 MV FFF	6 x 6	1.153
	10 x 10	1.219
	15 x 15	1.346
	20 x 20	1.499
	30 x 30	1.820

Source: The Author (2026).

Regarding the unflatness values calculated with the SH definition, the largest difference found for the 20 cm x 20 cm field was 1.4 mm in the $X_{60\%}$ value for the 6 MV FFF beam in Pichandi et al. (2014), which is below the 2 mm tolerance recommended by SH. To enable comparison with literature values, a triangle similarity relationship derived from the geometric divergence of the beam was applied to convert the lateral coordinate x of the profile measured at SSD 100 cm to the SAD 100 cm condition at a depth of 10 cm. Thus, the relationship $x(ssd\ 90) = 0{,}909x(ssd\ 100)$ was applied.

Table 6. Field sizes obtained for different methodologies across various field sizes for 6 MV FFF and 10 MV FFF beams, and the difference between the obtained and nominal field values (Diff).

	Field size (cm²)	Nominal (110 cm)	FG (cm)	Diff (mm)	SH (cm)	Diff (mm)	BDG (cm)	Diff (mm)
6MV FFF	6 x 6	6.60	6.56	-0.40	6.53	-0.70	6.54	-0.60
	10 x 10	11.00	10.99	-0.10	10.92	-0.80	10.97	-0.30
	15 x 15	16.50	16.52	0.20	16.43	-0.70	16.48	-0.20
	20 x 20	22.00	22.05	0.50	21.98	-0.20	22.01	0.10
	30 x 30	33.00	33.06	0.60	32.94	-0.60	33.03	0.30
10 MV FFF	6 x 6	6.60	6.53	-0.70	6.52	-0.70	6.53	-0.70
	10 x 10	11.00	10.99	-0.10	10.94	-0.60	10.97	-0.30
	15 x 15	16.50	16.49	-0.10	16.43	-0.70	16.46	-0.40
	20 x 20	22.00	22.04	0.40	21.99	-0.10	22.01	0.10
	30 x 30	33.00	33.07	0.70	32.95	-0.50	33.04	0.40

Source: The Author (2026).

Table 8. Unflatness values obtained using the SH methodology for different field sizes and 6 MV FFF and 10 MV FFF beams.

	6 MV FFF			10 MV FFF		
Field size (cm^2)	$X_{90\%}$ (cm)	$X_{75\%}$ (cm)	$X_{60\%}$ (cm)	$X_{90\%}$ (cm)	$X_{75\%}$ (cm)	$X_{60\%}$ (cm)
6 x 6	5.40	6.00	6.32	4.83	5.87	6.24
10 x 10	8.24	10.26	10.66	6.39	9.82	10.49
15 x 15	10.00	15.32	16.02	6.86	12.94	15.65
20 x 20	10.94	19.01	21.36	7.01	13.86	20.17
30 x 30	11.60	22.09	31.00	7.14	14.12	23.17

Source: The Author (2026).

Furthermore, it was found that the FG unflatness degree increases with beam energy and field size, as the elevation of these parameters intensifies the dose gradient in the central region of the beam. In contrast, the SH unflatness increases with field size and decreases with energy, as the profile becomes steeper, thereby reducing the lateral distance between the 90%, 75%, and 60% dose levels. Finally, among the evaluated methodologies, the FG definition proved to be simpler to analyze and closer to the values found in the literature.

3.5 Comparison between methods

The FG, SH, and BDG methods presented similar results for the evaluated dosimetric parameters, including field size, penumbra, and symmetry, with all values remaining within the established clinical tolerances. The FG method, although the most complex among the three, has its application facilitated by the use of tabulated NF values available in the original paper, and shown at Table 1. However, these values are only valid for the linear accelerators investigated in that study. Furthermore, this method relies on the use of conventional beams for the analytical derivation of the factor, which may be a limitation for centers that exclusively have accelerators with FFF energies. The BDG method proved to be the simplest to execute; however, by normalizing the profile, it ends up de-characterizing the FFF beam, making it equivalent to a conventional beam. In turn, the SH method has easy concepts and preserves the intrinsic characteristics of FFF profiles. Nevertheless, since the IP (inflection point) is located near 50% of the profile, in a high-gradient region (~10%/mm). Therefore, detector size and measurement step are critical factors, as insufficient resolution may lead to uncertainties in the determination of IP position and derived parameters, this method requires very small measurement steps for precise determination.

Finally, in this study, the SH method proved to be the most practical for application, as the obtained parameters showed good agreement with the literature, making it the most suitable for the routine of an institution that will operate linear accelerators from different manufacturers. The data obtained in this work will be used as a baseline for future profile measurements on the linear accelerator.

5. Conclusion

Three methodologies were evaluated for the characterization of flattening filter-free (FFF) photon beams. The results showed good agreement across all methods for key parameters, with field size differences within ±1.2 mm, penumbra variations below 0.7 mm, symmetry values below 1%, and unflatness differences below 0.7% for the FG definition and within 1.4 mm for the SH definition. For the BDG method, the derived profiles showed sub-millimeter agreement with conventional flattened beam parameters, consistent with values reported in the literature (within approximately ±0.5 mm).

The FG method was found to be precise and straightforward to apply using tabulated normalization factors (NF), whereas the BDG method, despite its simplicity, alters the intrinsic properties of the FFF beam. The SH method, in contrast, preserves the original characteristics of the FFF profile while remaining easy to implement. Consequently, the SH method emerged as the most suitable for routine clinical application. Its adoption

enables reliable and consistent characterization of FFF beams, enhancing quality control procedures. Given the unique properties of FFF beams compared to conventional beams, this methodology supports improved treatment safety and greater consistency in clinical quality assurance processes.

References

1. Pönisch F, Titt U, Vassiliev ON, Kry SF, Mohan R. Properties of unflattened photon beams shaped by a multileaf collimator. Med Phys. 2006 Jun;33(6):1738-46.
2. Vassiliev ON, Titt U, Pönisch F, Kry SF, Mohan R, Gillin MT. Dosimetric properties of photon beams from a flattening filter free clinical accelerator. Phys Med Biol. 2006 Apr 7;51(7):1907-17.
3. Cashmore J. The characterization of unflattened photon beams from a 6 MV linear accelerator. Phys Med Biol. 2008 Abr 7;53(7):1933-46.
4. Klein EE, Hanley J, Bayouth J, Yin FF, Simon W, Dresser S, et al. Task Group 142 report: Quality assurance of medical accelerators. Med Phys. 2009 Sep;36(9):4197-212.
5. Fogliata A, Garcia R, Knöös T, Nicolini G, Clivio A, Vanetti E, et al. Definition of parameters for quality assurance of flattening filter free (FFF) photon beams in radiation therapy. Med Phys. 2012 Oct;39(10):6455-64.
6. Sharma SD, Sahani G, Dash Sharma PK, Deshpande DD, Negi PS, Sathianarayanan VK, et al. Acceptance criteria for flattening filter-free photon beam from standard medical electron linear accelerator: AERB task group recommendations.J Med Phys. 2014 Oct-Dec;39(4):206-11.
7. Budgell G, Berresford J, Bunce C, Davies J, Flynn S, Hardy M, et al. IPEM topical report 1: guidance on implementing flattening filter free (FFF) radiotherapy. Phys Med Biol. 2016 Dec 21;61(24):8360-94.
8. Khan, F. M. The Physics of Radiation Therapy. 3 edition. Philadelphia: Lippincott Williams & Wilkin, 2010. 44-45.
9. International Atomic Energy Agency. Absorbed dose determination in external beam radiotherapy. Vienna: IAEA; 2000. (Technical Reports Series No. 398).
10. Glide-Hurst C, Bellon M, Foster R, Altunbas C, Speiser M, Altman M, et al. Commissioning of the Varian TrueBeam linear accelerator: A multi-institutional study. Med Phys. 2013 Mar;40(3):031719.
11. Clivio A, Belosi MF, Cozzi L, Nicolini G, Vanetti E, Bolard G, et al. On the determination of reference levels for quality assurance of flattening filter free photon beams in radiation therapy. Med Phys. 2014 Jan;41(1):011711.
12. Pichandi A, Ganesh KM, Jerina A, Balaji K, Kilara G. Analysis of physical parameters and determination of inflection point for Flattening Filter Free beams in medical linear accelerator. Rep Pract Oncol Radiother. 2014 Sep-Oct;19(5):322-31.
13. Bueno KP. Controle de qualidade em feixes de fótons de megavoltagem de alta intensidade, flattening filter free (FFF) [dissertação]. Recife: Universidade Federal de Pernambuco; 2017.
14. Sharma S, Dixit DK, Sharma SD, Sharma A, Sahani G, Upreti RR, et al. A Simplified Approach for Determination of Inflection Points of Flattening Filter-Free Photon Beam Using In-House Developed Software and Derivation of Reference Levels. J Med Phys. 2023 Jul-Set;48(3):259-67.
15. Furnari, L. Controle de qualidade em radioterapia. Crayon Editorial, 2021. 624-625

Contact:

Camila Soares Aguiar
School of Medicine of the University of São Paulo, São Paulo, Brasil
Av. Dr. Arnaldo, 455- Cerqueira César, Pacaembu, SP
camila.saguiar12@gmail.com